ELSEVIER

Polymer 43 (2002) 3267–3277

polymer

www.elsevier.com/locate/polymer

Morphology development in polymer blends produced by chaotic mixing at various compositions

D.A. Zumbrunnen*, C. Chhibber

Department of Mechanical Engineering and the NSF Center for Advanced Engineering Fibers and Films, 214 Fluor Daniel Building, Clemson University, Clemson, SC 29634-0921, USA

Received 7 September 2001; received in revised form 25 January 2002; accepted 31 January 2002

Abstract

Whereas blending devices commonly entail complex flow fields and internal geometries, chaotic mixing can be instilled by simple periodic motion of bounding surfaces in simple devices. Breakup and coalescence of spatially expansive structures in components can give blends with a wide variety of morphologies. In this study, polystyrene and low density polyethylene were used as model components to study the effect of composition and processing time on gradual morphology development in immiscible binary blends. Inspections of samples disclosed attainable morphologies and also how transitions between morphologies occurred. Novel findings included blends with encapsulated fibers, abundant platelets, and two distinct morphologies having single phase continuity. Additionally, interpenetrating blends formed over a broad compositional range. Results suggest that chaotic mixing is a useful tool for studying relationships among processing conditions, morphology development, and blend properties and may serve as a means to more deliberately obtain target morphologies.

Keywords: Morphology; Chaotic mixing; Blends

1. Introduction

Like any composite material, specific shapes and size scales for polymer components are often sought in immiscible blends in order to enhance performance. For example, where permeation resistance is important, a blend that consists of many thin platelets is preferable to one containing droplets. In most polymer processing equipment, blend morphology is an outcome of an interplay among flow conditions, breakup and coalescence. Consequently, composition strongly influences morphology and the variety of attainable morphologies are often limited. Degradation of ancillary properties can occur as a target morphology is pursued by increasing the content of one component. To produce platelet or fibrous morphologies, intermediate compositions are sometimes necessary such that large bodies arise from significant coalescence during compounding that can be readily extended due to their size during extrusion steps. The coupling between morphology and composition, the rapidity of morphology changes, and the complexity of time-varying flow fields in most polymer processing equipment represent substantial obstacles to researchers investigating structure–process–property relations and validating computational models. In this study, chaotic mixing is employed to produce a wide variety of blend morphologies and study gradual transitions from one morphology to another. Results suggest that chaotic mixing may serve as a basis for blending processes where morphology development can be more readily controlled to give target morphologies.

It is commonly misunderstood that processes based on chaotic behavior are uncontrollable. While it is true that the physical locations of particular blend features within a chaotic mixing device are sensitive to even minute process variations, blend morphologies are consistently reproducible and their development can be controlled by simply adjusting process duration or parameters related to chaotic mixing. Aref [1] articulated that fluid particles can undergo complex motions in response to simple periodic agitations and dubbed the phenomenon as *chaotic advection*. Because fluid domains are stretched and folded recursively, chaotic advection has been implemented principally as an effective means to model mixing. Mixing studies that make use of chaotic advection consequently often employ the term, *chaotic mixing* [2]. Interestingly, simple laminar and periodic fluid flows can give rise to chaotic motion among fluid particles. Key aspects of blending processes can be

* Corresponding author. Tel.: +1-864-656-5625; fax: +1-864-656-4435.
E-mail address: zdavid@ces.clemson.edu (D.A. Zumbrunnen).

0032-3861/02/$ - see front matter
PII: S0032-3861(02)00139-8

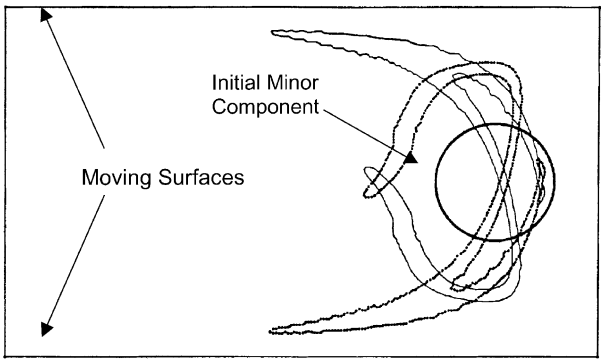

Fig. 1. Computational simulation of stretching and folding of a circular minor component body due to sequential motions of upper and lower walls in a simple chaotic mixing device [3].

obtained such as shear induced deformation and reorientation of fluid domains, and devices can be comparatively simple in design. This situation is depicted in Fig. 1 [3], where a circular minor component body and a major component melt are located in a rectangular cavity that has been used in many chaotic mixing studies [4,5]. In response to the sequential lateral motions of the upper and lower cavity surfaces and associated shear flows, the circular body has been stretched and folded. Separate morphology changes have been overlaid that were in response to forward and reverse mappings. Continued chaotic mixing would act recursively on refined and more complex shapes so that hierarchical associations among structures may arise with relation to some natural materials [6,7].

Because chaotic mixing can occur in response to simple programmed motions of bounding surfaces, morphology development occurs progressively. In a related study [8], polymer melt streams were supplied at steady and prescribed rates to a chaotic mixing device consisting of a barrel and internal stir rods. The motion of the rods was selected to induce chaotic advection. Stretching and folding acted for longer times at points more distant from the entrance point so that sheets refined to give extrusions with a multilayer morphology and specified number of internal layers. As will be shown, morphology transformations in the layers may yield other useful blend morphologies. In essence, other blend morphologies are obtained from highly multilayered structures by decreasing interfacial area among components in natural or induced transitions. Chaotic advection has been demonstrated in other continuous flow devices, such as twisted pipes [9] and enclosed wavy channels [10]. While these devices can provide new means for fluid mixing, they offer less opportunity for controlling blend morphology than do configurations where the motions of internal stir rods or bounding surfaces can be specified.

As suggested in Fig. 1, blends produced in chaotic mixing devices can have spatially expansive structures in contrast to blends produced in screw extruders where small flow passages and complex flow fields actively break down structures to reach a well-mixed condition often consisting of droplets. Spatially expansive structures with small-scale features such as very thin layers can undergo morphology transitions that lead to other spatially expansive structures. *Progressive morphology development*, where one morphology leads to another morphology in sequence, provides a means for obtaining a wide variety of blend morphologies [11]. While similar morphology development may arise in conventional equipment, it often occurs only within small regions or for short time intervals in contrast to more expansive regions and longer durations in chaotic mixing devices. For example, low density polyethylene (LDPE) or poly-[ethylene-stat-vinyl acetate] (EVA) as minor components have been blended with polystyrene in a batch process by three-dimensional chaotic mixing at a single composition of 25 vol% [12]. Beginning from a random mixture of melted resin pellets to give good initial compositional uniformity, abundant sheets and films were formed in the LDPE and EVA phases, that upon continued chaotic mixing, developed instabilities. The instabilities in films of large spatial extent yielded long fibers with diameters similar to the parent film thicknesses. Similar morphology development and morphology transitions were documented in a blend of 9% LDPE and PS [13]. Blends were readily produced with a wide variety of morphologies since samples could be produced after a selected degree of morphology development. The impact toughness of PS was improved by 69% due to the presence of the structured LDPE component, whereas impact toughness was degraded for the droplet morphology. Blending processes that inherently evolve structure among components can be used to manufacture plastics with enhanced properties. As pointed out by Teh and Rudin [14], mechanical properties such as impact toughness of PE/PS blends that are produced by common compounding methods are rarely better than those of pure PS.

Morphology development for conditions in screw extruders and batch intensive mixers is an active subject of ongoing research. It is important to note that much of the complexity in understanding morphology development arises due to complexities inherent in the blending devices themselves. Because the basis for screw extruders is the transfer of very viscous melts, their application to multicomponent polymer systems and mixing yields a rapid and essentially uncontrollable sequence of morphology changes. In contrast to the chaotic mixing process of this study, resin pellet mixtures are often simultaneously sheared, heated, melted, and interspersed. Interfacial structures, which define a blend morphology, are rapidly evolved and broken down. To clarify early behavior, initial morphology development was studied where a minor component pellet was sheared at controlled rates between rotating disks at fixed composition [15]. Sheets were formed that rapidly developed numerous holes. Hole growth led to a tenuous structure consisting of ligaments that broke to give droplets. It was noted that results described how resin pellets in twin screw extruders break into sub-micron

particles for residence times of only a few seconds. Morphology development, also at fixed composition, was documented for more complex flow conditions in a batch intensive mixer by quenching removed samples in liquid nitrogen [16]. A sequence of morphology changes was described where sheets or ribbons developed holes that enlarged to yield a lace-like structure. These subsequently fragmented to give cylinder and droplet shapes.

Schreiber and Olguin [17] investigated blends of polypropylene (PP) with dispersed phases of polystyrene, ethylene–propylene rubber and bromo-butyl rubber produced in an extruder. It was observed that mean droplet radius decreased to a limiting value with increased mixing time so that continued mixing was unproductive. Karger-Kocsis et al. [18] conducted a morphological study of PP/ethylene–propylene–diene terpolymer (EPDM) and PP/polyolefin thermoplastic rubber blends. No considerable improvement in the degree of dispersion was achieved by increasing mixing duration greater than about 5 min. Very little reduction in the size of the dispersed phase in PP/polycarbonate blends was found at various shear rates by extending mixing times [19]. The most significant changes in morphology occurred during the first 2 min of mixing when melting and softening of the materials was also occurring. These studies differed from the present study where blend morphology was developed only in the melt state and fine-scale dispersed morphologies were obtained from the breakup of thin multiple film layers.

Much as batch mixers are used to study morphology development in extruders, this study employed a batch chaotic mixer to elucidate the types of blend morphologies and morphology transitions that can occur in continuous flow chaotic mixers [8]. The influence of composition on morphology development was specifically investigated. A wide variety of blend morphologies was generated with many formed at single compositions. Similar morphologies were also obtained at different compositions through control of chaotic mixing parameters. Because processing conditions differed from those of conventional equipment, novel blend morphologies were also obtained in some instances.

2. Experimental methods

2.1. Chaotic mixing apparatus

Blending was performed in a batch three-dimensional chaotic mixer that was specifically developed for blending studies. Unlike cavities that have been used in chaotic mixing investigations where fluid mixing was the focus, the eccentric disk chaotic mixer (EDCM) allowed easy removal of solidified specimens since it contained no internal parts such as impellers or rods. Conditions for inducing chaotic mixing throughout the internal volume of the EDCM were established through computational simulations

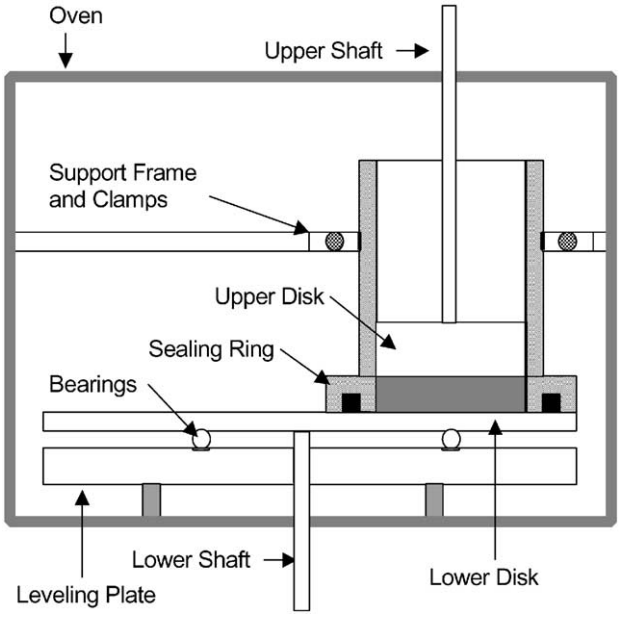

Fig. 2. Schematic diagram of the EDCM developed for blending studies.

that were experimentally validated using pigmented Newtonian fluids as well as thermoplastics [20]. The EDCM, which was placed inside a convection oven, was formed within a stationary vertical stainless steel cylinder of inner diameter $D = 51$ mm and with upper and lower horizontal stainless steel disks, as shown in Fig. 2. Motion in the melt was instilled by separately and periodically rotating each disk by a specified angular displacement via upper and lower shafts that extended into the oven. Morphology development was therefore predominantly in response to shear flows that were separately active. Because the rotational axis of the lower disk was offset from the cylinder axis, rotations caused a cross-flow that was deflected by both the cylinder wall and upper disk. The upper disk induced a simpler rotational flow about its axis. Leakage from the melt along the lower disk was prevented by a labyrinthine nylon seal ring inserted in the base of the cylinder. A leveling plate and precision ball bearings ensured that the seal maintained close contact during rotations of the lower disk. A small gap between the upper disk and cylinder wall prevented mechanical binding while also allowing the escape of gases during melting.

The vertical height H of the EDCM was adjustable by either inserting or retracting the upper disk within the cylinder. Specimens can be produced over a range of aspect ratios $A(= H/D)$. Also, the radial distance E between the axes of the upper and lower shafts is adjustable to allow specification of the axis eccentricity $e(= 2E/D)$. In this study, $A = 0.1$ and $e = 1.6$. For this small aspect ratio, each disk motion effectively propelled melt throughout the cavity volume and thin specimens were more rapidly solidified. The large eccentricity placed the rotational center of the lower disk outside the cavity and provided nearly orthogonal intersections between flow pathlines associated

with the disk motions for more effective chaotic advection. In general, smaller periodic rotational displacements are needed to give chaotic advection throughout the EDCM volume for larger eccentricities and smaller aspect ratios [20]. The disk rotations were provided by separate servo-motors and were controlled via a programmable digital motion controller. A rotational speed of 2 rpm was used for both disks. The extent of morphology development was related to the number N of chaotic mixing periods, where one period comprised one separate and sequential rotation of the upper disk and lower disk. When viewed from above, the lower disk was rotated counter-clockwise followed by the clockwise rotation of the upper disk. The fraction of a complete rotation for each disk during one period was defined as the perturbation strength μ. In this study, $\mu = 0.6$. While chaotic advection can occur in steady three-dimensional flows, a time-periodic flow field was implemented since greater opportunity for morphology control was provided. For example, both μ and N can be specified in lieu of only elapsed processing time.

Because the disk rotational speed was small, disk displacements occurred over several seconds and greatly exceeded the characteristic relaxation times of typical thermoplastics. Reynolds, Deborah, and Weissenberg numbers were estimated to be below 10^{-1}. As such, inertial and viscoelastic effects were small. Stokes flow conditions prevailed throughout the cavity. Such flows have pathlines that are wholly determined by the motion of bounding surfaces and geometry. Fluid motion and morphology development are qualitatively identical for cavities of different size. For example, the layered morphologies in Fig. 1 would appear in both small and large chaotic mixing devices. Viscoelasticity has caused secondary flows in the form of spiral vortex tubes in a related cylindrical cavity with a concentric rotating lower disk [21]. While dispersion was improved, secondary flows were undesirable in this study since coherent flow structures can impede progressive morphology development and restrict the spatial extent of evolving bodies. The influence of disk rotational speed on morphology development with the EDCM was performed in a prior study [13]. Little effect was noted for speeds below 2 rpm.

2.2. Materials and processing conditions

Polystyrene (PS) and LDPE were selected as components for a model immiscible blend and for consistency with a recent study where morphology development by chaotic mixing was reported at a single composition of 9 vol% [13]. Atactic polystyrene (GPPS 555, Nova Chemicals, Inc., Calgary, Alta., Canada) and LDPE (18 BOA, Eastman, Inc., Kingsport, TN, USA) in the form of pellets were used. Local shear rates that corresponded to the separate motions of the upper and lower disks ranged from 0–1.02 to 0.07–2.75 s^{-1}, respectively. Viscosities were measured with a cone and plate viscometer (RMS-800, Rheometric Scientific, Piscataway, NJ, USA) in the low shear rate range at the processing temperature of 190 °C. The viscosity ratio (LDPE/PS) varied from 0.07 to 0.3 over the applicable shear rate range. Results are summarized in Fig. 3. Viscosity ratios were lower in cases where the LDPE was the minor component so that flows within minor component bodies became organized more quickly to give more rapid morphology transitions [3,22,23]. The surface tension values for LDPE and PS were adopted from the work by Sanchez [24]. The interfacial tension between LDPE and PS was determined to be 4.5 mN/m according to methods of Willemse et al. [25]. The transition temperatures were measured by differential scanning calorimetry at a heating rate of 10 °C/min. The glass transition temperature of PS was 81 °C and the melting temperature of LDPE was 114 °C.

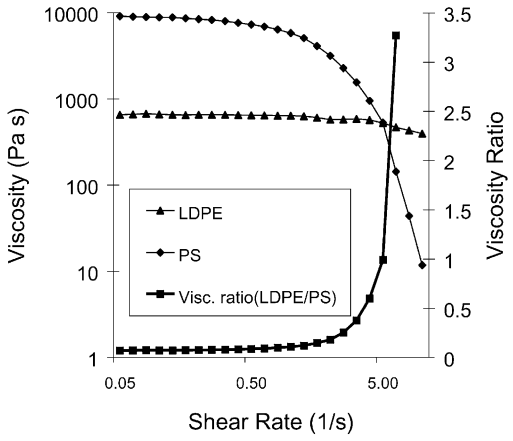

Fig. 3. Viscosity and viscosity ratio for PS and LDPE.

Polymer pellets were carefully weighed using a precision digital mass balance to give the required composition. The weighed portions were combined by mechanical shaking to yield a pellet mixture with good initial compositional uniformity. This approach was found to be most effective where melt structuring is the focus since morphology development by chaotic mixing can occur more rapidly than component distribution. Seven different weight compositions of the PS/LDPE blends were considered (i.e. 10/90, 20/80, 30/70, 50/50, 70/30, 80/20, 90/10). To begin an experiment, pellet mixtures were poured into the mixing cavity and the oven was energized. After 1 h, the upper disk was lowered with an external linear positioner to contact the melt. Chaotic mixing was begun 30 min later, with the lower disk rotating first as described earlier. After the prescribed N, the oven was de-energized and the cavity was cooled within 10 min below the glass transition temperature of PS using a compressed air jet. Cooling was continued for ten additional minutes so the cavity could be removed by hand. A hand press was used to remove the sample from the cavity.

2.3. Morphology evaluation

Samples were cut to extract rectangular specimens

10 mm from the sample center with lower sides parallel to the disk surfaces. The samples had square cross-sections with 10 mm sides and were 20 mm long. Specific planes and immiscible components within samples were exposed by immersing samples in liquid nitrogen and fracturing along notched surfaces. Due to poor interfacial adhesion between the immiscible polymer pair, internal structure was made evident by the fracturing step and by use of a field emission scanning electron microscope (Model 4700, Hitachi, Tokyo, Japan). The FE-SEM eliminated the need for gold coating and was capable of discerning blend components. To examine more thoroughly the LDPE morphology by FE-SEM, the PS was removed from some samples by soaking in toluene at room temperature.

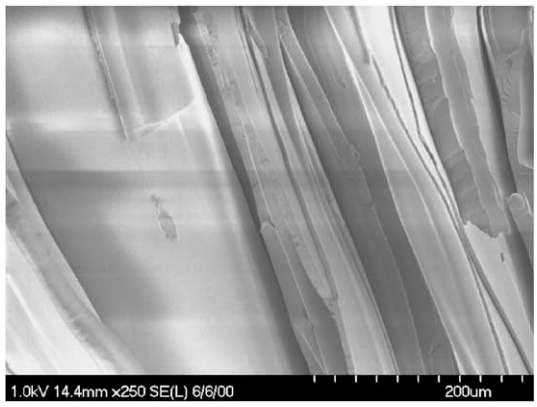

Fig. 4. Sheets produced in blends with 20% PS and $N = 6$.

3. Results and discussion

3.1. Initial morphology development (sheets and incipient structures)

Morphology development over the entire compositional range was investigated by producing samples for increasing processing times given in terms of the number N of chaotic mixing periods described earlier. Representative examples of morphologies at specific compositions will be supplemented with descriptions of morphologies at other compositions. All morphologies are summarized subsequently in a diagram showing process conditions. For $N < 5$, the initially coarse dispersion of molten PS and LDPE pellets within the chaotic mixer was converted at all compositions to alternating sheets. Because flows were predominantly parallel to the disk surfaces (Fig. 2), clear views of individual layers were obtained by viewing vertical cross-sections of samples. Multiple and distributed sheets were evident for $N = 2$ in a specimen with a composition of 80% PS. Due to the higher PS viscosity (Fig. 3), a longer processing time of $N = 6$ was required to obtain similar structures shown in Fig. 4 at the inverse composition of 20% PS. In lieu of the single minor component body of Fig. 1, chaotic advection acted on the initial dispersion of LDPE and PS pellets within the cavity. In general, both the LDPE and PS components became stretched and folded about each other as chaotic mixing proceeded to produce an alternating sheet morphology. The influence of viscosity ratio and interfacial tension on evolving film layers has been studied computationally [3]. It was found that similar structures can be formed at inverse viscosity ratios if greater processing time is allowed where viscosity ratios exceed unity. The similarity of the layered structures was consistent with the computational simulations. As a physical explanation taken from the simulations, the layered structures evolved from initially large bodies. The ratio of shear stress forces to interfacial tension forces for such bodies were thereby large so that bodies deformed readily. This situation is analogous to the deformation of large droplets when capillary numbers exceed a critical value. Because stretching and folding (Fig. 1) caused interfacial areas to increase, subsequent deformations by the imposed shear were more easily achieved than the initial deformations.

In Fig. 5, folds and undulations are shown in layers with thicknesses of about 20 μm. In the absence of breakup, the shapes of structures increased in complexity as processing proceeded. Additional stretching and folding of these complex shapes enhanced distributive mixing such that compositional uniformity was attained at smaller length scales. Folding also caused the mutual envelopment of one component by the other in some locations. As will be shown, envelopment eventually yielded novel encapsulated structures. This characteristic of chaotic mixing was distinctly different from what occurs in simple flows such as pure shear or extensional flows. In static mixers and layer multiplication dies, component distribution or creation of layered structures are achieved by splitting and reorienting a flow with stationary elements [26]. In contrast, Figs. 4 and 5 demonstrate that a similar process can be achieved in chaotic mixing devices with moving surfaces. In these devices, the extent of melt structuring is selectable through N or by choice of other parameters, such as μ [8].

Fig. 5. Folding and incipient phase encapsulation associated with chaotic advection in a sample with 20% PS and $N = 6$.

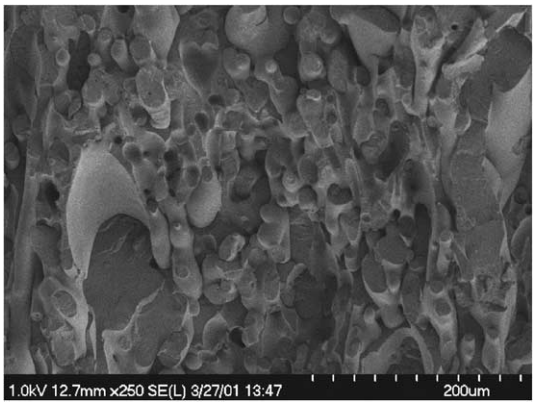

Fig. 6. Interpenetrating blend formed with 35% PS and $N = 10$.

3.2. Intermediate morphology development (hole formation, interpenetrating blends and fibers)

For $5 < N < 15$, several distinct morphologies were obtained with some achievable at identical compositions. An example of an interpenetrating blend with 35% PS is shown in Fig. 6. Similar morphologies were obtained over a wide 35–90% PS composition range although the extent of connectivity within each component remains a subject of ongoing study. The example in Fig. 6 was therefore a limiting case. A more typical IPB morphology is shown in Fig. 7 for 80% PS where the PS component was removed by dissolution in toluene. To confirm the IPB morphology, the mass of the sample was measured before and after dissolution. Results indicated that all of the PS had been extracted. The toluene was able to reach all interior portions of the sample through the interpenetrating structure. When manipulated by hand, the sample had a spongy response and recovered its initial shape. Obtaining interpenetrating blends from simultaneous hole formation in blends with layered morphologies formed by two-dimensional chaotic mixing was also recently documented at a single composition of 6.4 vol% LDPE and PS [27].

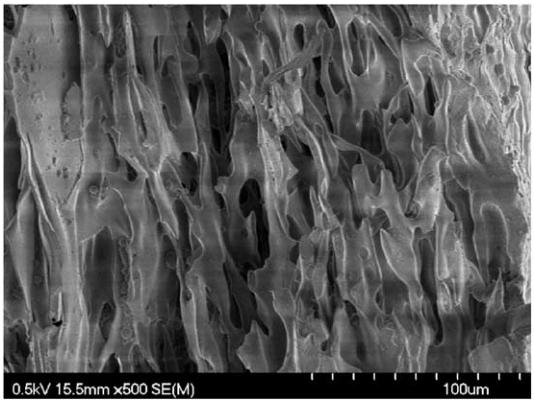

Fig. 7. Interconnected LDPE structures in an interpenetrating blend after removal of a continuous PS component by dissolution for 80% PS and $N = 10$.

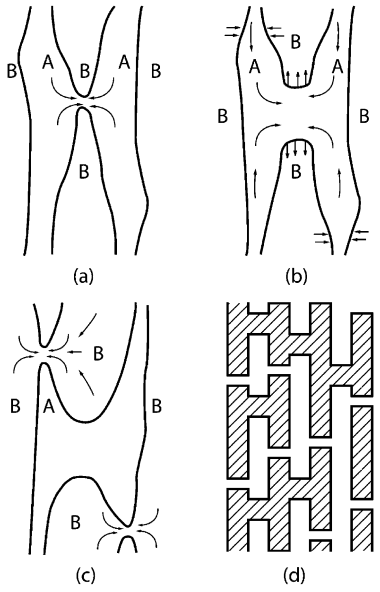

Fig. 8. Interactive hole formation in blends with multilayer morphology and emergence of an interpenetrating blend: (a) incipient hole formation in region of smallest layer thickness; (b) hole enlargement and adjacent layer thinning; (c) incipient hole formation in layers of other component; (d) multiple holes leading to phase continuity.

The wide compositional range for the formation of IPBs occurred because all were derived from the parent alternating sheet morphology formed initially at all compositions, such as those shown in Figs. 4 and 5. The transition from a sheet morphology to an IPB morphology is depicted in Fig. 8. With further stretching and folding, ruptures eventually occurred in regions where layer thickness was smallest. In Fig. 8(a), for example, a rupture in a layer of polymer B is shown. With the rupture, melt from previously separated layers of polymer *A* coalesced. Unlike in layers with less distortion and of more uniform thickness where circular holes have been documented [15,28], the ruptures in layers of nonuniform thickness led to elongated holes with major axes oriented along the directions where layers were thinnest. In Fig. 8(b), melt was drained from the thicker adjacent polymer *A* layers. Hole growth in the *B* layer and melt drainage caused the adjacent *A* layers to become thinner. Consequently, ruptures also eventually occurred in the adjacent *A* layers at points where the layers were initially thinner (Fig. 8(c)). Thus, hole formation in layers of both components was hastened by nonuniformities in layer thicknesses. Nonuniformities were outcomes of the chaotic mixing process as evident in the computational result of Fig. 1. Flow interactions among the layers occurred such that the thicknesses of layers with holes decreased less rapidly or perhaps even increased, while the decrease in thicknesses of intact layers was accelerated. Through this interplay, hole formation in the layers of one component promoted hole formation in layers of the other component to yield the interpenetrating blend shown in Fig. 8(d). (This formation mechanism has been recently

demonstrated in computational simulations that will be reported in a future paper.)

The novel route for obtaining an IPB morphology of Fig. 8 yielded an IPB over a compositional range much broader than provided by a widely used condition for dual phase continuity [29], $\eta_1(\gamma)/\eta_2(\gamma) \approx \phi_1/\phi_2$, where 1 and 2 denote the blend components, η is viscosity, γ is the actual shear rate present in the mixing device, and ϕ is the volume fraction. The chaotic mixing processing method allowed control of layer refinement and extent of hole growth by simple designation of the number N of pairs of disk motions. It is unlikely that the IPB formation route of Fig. 8 would be observed in multilayer films produced with layer multiplication dies. In these devices, the number of layers is increased by dividing and stacking a melt stream. For two initial layers, the number of layers increases according to 2^n, where n is the number of layer multiplication stages. If hole formation is not observed for a particular n, an additional stage can cause complete layer breakup. For example, if 1024 intact layers are formed for $n = 10$, an additional stage would yield 2048 layers. This large incremental increase in the number of layers and the associated refinement in layer thickness may be unachievable. With chaotic mixing devices, layer refinement can be readily controlled to focus on a target morphology transition and allow hole growth to progress to a desired degree. Similarly, this morphology development may not be observable in screw extruders where structure is rapidly broken down.

In addition to promoting the formation of interpenetrating blends, the stretching and folding of sheets and appearance of holes were also associated with the formation of fibers. Fiber formation from sheets in shear flows has been attributed to normal stress differences arising at high shear rates [15]. However, in this study where sheets were subjected to stretching and folding related to chaotic advection, differing morphologies from sheet breakup were obtained at the same low shear rate levels. The central importance of hole formation and growth were evident in micrographs and are summarized in Fig. 9. Very localized layer thickness variations, such as those in Fig. 8 associated with IPB formation, promoted the formation of circular and elliptical holes. Hole growth and elongation in a layer occurred preferentially along the direction where layer thickness was smallest. The cumulative elongation was related to the length of the thickness variation. For example, point depressions led to circular ruptures whereas line segment depressions led to elongated ruptures. The proximity of many elongated holes was only possible, however, if orientation among the line segment depressions also arose. Orientation among many depressions led to the formation of long parallel thickness undulations. Just as holes formed at point depressions, hole growth along line depressions in layer undulations yielded multiple fibers. An example of a layer with such instabilities is evident in the center of Fig. 10. LDPE fibers that were derived from sheet breakup are shown in Fig. 11 for a blend of 92% PS. As a result of fracturing specimens to expose

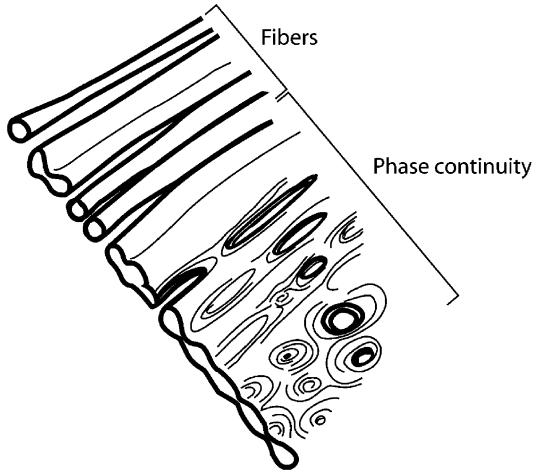

Fig. 9. Relation of layer thickness variations to derivative morphologies.

internal morphology, portions of fibers and depressions left by fibers were indicated in micrographs. PS fibers were similarly present in the inverse blend of 92% LDPE. Fiber diameters of about 4 μm were similar to the thicknesses of parent layers. Because the wavelength of undulations in layers was similar to the layer thickness, numerous fibers were obtained from the breakup of each layer. The direct conversion of layers to fibers by chaotic mixing in other blends was also reported in a prior study [12]. Blends were produced at the single composition of 25 vol% EVA and LDPE or 25 vol% LDPE and PS. Fibers were found with aspect ratios of about 300.

In addition to the single component fibers such as in Fig. 11, novel encapsulated fibers were also present in the binary blend whereas encapsulation is normally associated with blends of three or more components [30]. These novel structures have characteristics of both fibers and films, if one notes that an encapsulating layer can be regarded as a film surrounding an interior fiber. In Fig. 12, layers of LDPE and PS were folded about one another. Line rupture of the internal layer led to the coalescence of the outer layer with itself to yield an encapsulated fiber, such as the examples shown

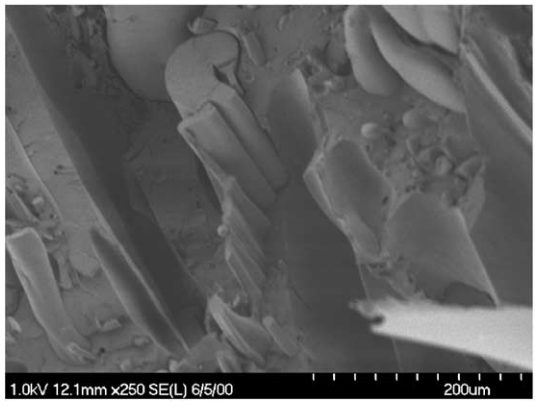

Fig. 10. Sheet breakup along line ruptures in a sample with 20% PS and $N = 14$.

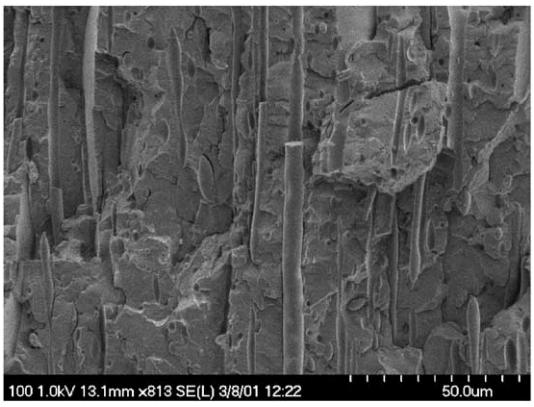

Fig. 11. Long fibers formed after line ruptures in a layer in a blend with 92% PS and $N = 14$.

in Fig. 13. This formation mechanism is illustrated in Fig. 14(a). Encapsulated structures can also be formed without coalescence events. Because minor and major component bodies became stretched into adjacent sheets such as shown in Fig. 4, alternating shear flows can become directed toward reorienting sheet surfaces. The sheet surfaces thereby can become arranged much like when a stack of cloth layers is raised by a fingertip (Fig. 14(b)). Numerous regions in chaotic mixing devices can be present where fluid moves predictably instead of chaotically. In such regions shown in Fig. 14(c) that have been dubbed 'islands' by investigators of chaotic mixing [2], melt circulates and remains segregated from adjacent regions where chaotic advection occurs. Encapsulation of components occurs. Interestingly, even when chaotic advection dominants a flow, the islands can be numerous and have dimensions of less than a few microns where interfacial tension is small [6]. The encapsulated structures may become elongated when subjected to extensional flows in extrusion steps to give internal fibers like those in Fig. 13 but with many levels of encapsulation. As is evident from Fig. 14, a variety of encapsulated structures and different levels of encapsulation can be present in blends formed by chaotic mixing.

In the foregoing morphologies, morphology development

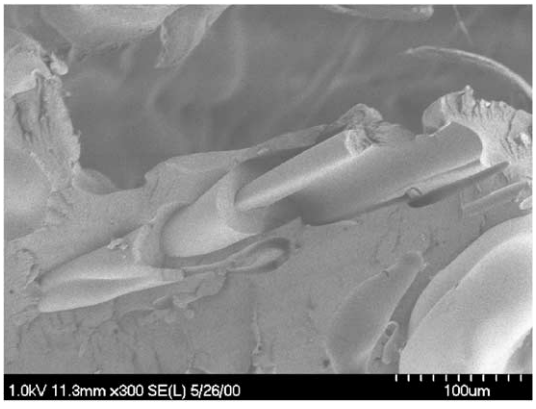

Fig. 12. Longitudinal instabilities in encapsulated sheets near folds for 20% PS and $N = 10$.

(a)

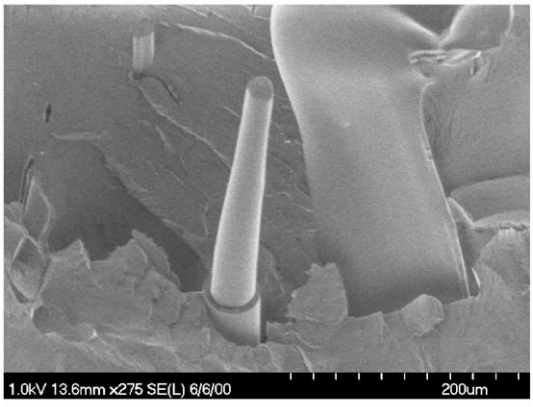

(b)

Fig. 13. Examples of encapsulated fibers: (a) 10% PS, $N = 10$; (b) 20% PS, $N = 6$.

was influenced by thickness variations in layers. These arose due to chaotic advection and interactions among component bodies. For time-periodic two-dimensional flows, for example, kinematical features such as in-flow and out-flow manifolds of hyperbolic points became tangled [2,31]. As a result, minor and major component bodies experienced over time both compression and extension with unique time histories and layers became buckled. Body interactions were generally more prevalent at intermediate compositions where interbody distances were smaller [3]. The influence of body interactions were compounded by continued chaotic mixing by stretching and folding shapes of greater complexity. Variations in layer thickness were more localized such that point depressions and holes were more apt to form than elongated ruptures associated with fibers. For this reason, fiber shapes were found only at high and low compositions.

3.3. Comments on hole formation mechanisms

The formation of holes in films is an active research area owing to its relevance to a wide variety of film processes and products. From the earlier results, it is evident that hole formation is very pertinent to blends produced by chaotic mixing where multiple layers initially form at all

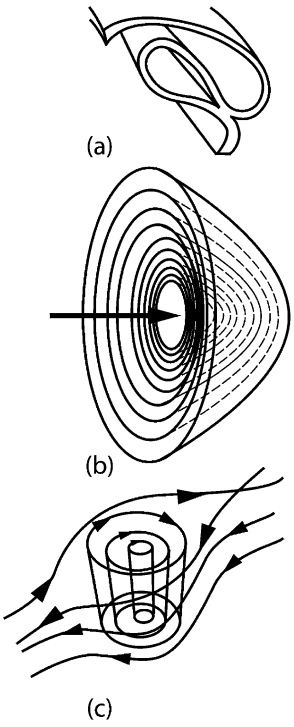

Fig. 14. Encapsulation mechanisms in chaotic mixing: (a) coalescence of folded layers; (b) deflection by flow of multiple layers upon reorientation; (c) small regions of regular motion surrounded by regions where chaotic advection occurs.

compositions. While a clear understanding of hole formation in multilayer films awaits further study, some insights can be discerned. Nearly all theoretical and experimental studies have considered hole formation in a single film layer in lieu of a large number of layers, such as shown in Fig. 4. It should be noted that 2 mm filaments have been extruded with more than 10 000 layers using a chaotic mixing device operated in a continuous flow mode [8]. An understanding of hole formation and other multilayer breakup modes (e.g. Figs. 8 and 9) can provide means to produce a variety of derivative blend morphologies in continuous flow chaotic mixing devices.

Analytically, it has been shown that a hole in an isolated layer can grow due to interfacial tension forces only when the hole diameter is large in comparison to the layer thickness [32]. Smaller holes, if formed, would collapse. Impurities such as particles must have diameters greater than the layer thickness to induce holes that can grow. In this study, large numbers of holes were found in layers as thick as 10 μm. While readily detectable by microscopy, impurities were not found. Hole formation in single polymer films on substrates has been attributed to the amplification of thermally excited waves by van der Waals forces. van der Waals forces increase rapidly as the distance between the free surface and the substrate decreases. Various studies have verified the importance of van der Waals forces on layer breakup. Separation distances between forming holes in a PS film on a ceramic substrate agreed with theoretical predictions where distances on average were in proportion to the square of the layer thickness [27]. Neutron reflection measurements of the buried interface between a poly (methyl methacrylate) film and a PS melt substrate have also been consistent with this hole formation mechanism [33]. However, for a single polymer layer located within a medium of another polymer, two deformable interfaces exist. It has been conjectured that oscillations in these interfaces may induce holes at the closest points of approach [15]. Whereas hole formation is often observed in single polymer films with thicknesses less than about 0.2 μm, the combined motions of two or more interfaces may partially explain why holes can form in thicker layers where multiple layers exist. Additional causes may stem from local thickness variations in layers induced by chaotic advection, as described earlier, and interfacial instabilities driven by shear forces. The breakup of relatively thick layers by hole formation has been attributed to the influence of localized film-thinning disturbances such as gravitational drainage or surface tension gradients [34]. Chaotic mixing and shear may similarly provide disturbances such that relatively thick layers can develop holes.

For the multilayer films of this study where layer thicknesses varied locally, van der Waals forces were greatest along point depressions or line deformations. As such, film breakup occurred by either point rupture (i.e. hole formation, Fig. 8) or line rupture (i.e. tears, Fig. 9). It has been pointed out that the mathematical correspondence between line ruptures in a sheet and capillary instabilities in a fiber is close for models that account for van der Waals forces [35]. Where multiple line ruptures in a film occur, many fibers may result in analogy to the numerous droplets derived from capillary instabilities. This route to fiber formation from multilayer blends has been documented in immiscible blends [12] and was also suggested by multiple, parallel line deformations in layers as in the central layer in Fig. 10.

3.4. Long-term morphology development (persistent IPBs, platelets and droplets)

In chaotic mixing, different morphologies were obtained through transitions from one morphology to another as N was increased. Long-term morphology development (e.g. $15 < N < 25$) was therefore influenced by prior morphology transitions. Within the range 75–85%, the IPB morphology such as shown in Figs. 6 and 7 that first appeared at about $N = 7$ remained present for $N = 25$, which was the highest number of mixing periods considered. This result indicated that the IPB was appreciably stable in the presence of the alternating shear flows in the apparatus of Fig. 2. The IPB morphology persisted for fewer numbers of periods at lower and higher compositions within the range for IPB formation of 35–90%. The growth of the numerous irregularly shaped holes in the IPBs resulted in fragmentation of either the continuous LDPE or PS phase and the formation of abundant platelets. The initial

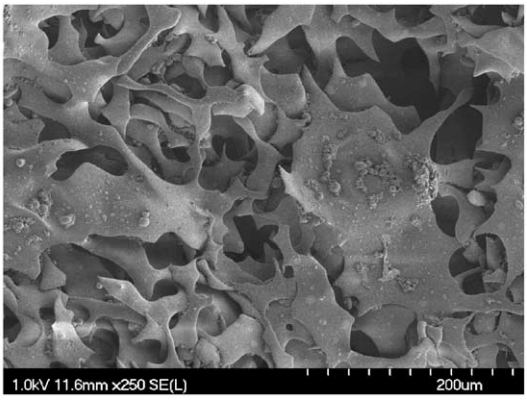

Fig. 15. LDPE platelets liberated by dissolution in a sample with 90% PS and $N = 20$.

formation of sheets as a means to create platelet morphologies was effective. An example of LDPE platelets in a sample of 90% PS is shown in Fig. 15, where the PS was removed by dissolution. The appearance of platelets in one component marked a transition to a blend with single phase continuity in the other component. As would be expected, platelets formed initially in the component with the thinnest layers and a corresponding lower concentration, although behavior was more complex at intermediate compositions where platelets of either component were possible due to layer thickness variations, differences in component viscosities, and flow interactions among layers. Interestingly, single phase continuity in a component was also present at shorter processing times due to the earlier formation of holes in the other component. Two distinct morphologies with single phase continuity were thereby producible: one with holes present in layers of one component and the other with platelets of the same component.

Capillary instabilities in fibers and fragmentation of platelets yielded droplet dispersions. Platelet fragmentation was due to the growth of interior holes. As described earlier, the continuing growth of holes occurred where hole diameters were greater than the layer fragment thickness [32]. Computational simulations have demonstrated that larger platelet fragments in alternating shear flows such as used in this study contracted due to interfacial tension to give thicker fragments and eventually larger droplets [3]. Very fine droplets were also evident that were the outcome of capillary instabilities and end-pinching of tendons interconnecting the enlarging holes associated with platelet formation. A range of droplet sizes reflected distinctly different formation pathways that included tendon fragmentation, relaxation of platelet fragments, and also coarsening due to coalescence. Recently, abundant droplets with diameters below 50 nm were produced in extrusions by a continuous flow chaotic mixing process in a blend consisting of PP and EPDM [36]. The droplet sizes were about two orders of magnitude below those of droplets resulting from fragmentation of extended bodies in shear flows [37]. Diameters were related to the thicknesses of parent film layers. In these layers, numerous closely spaced holes were documented. As a result, hole growth and layer fragmentation yielded multitudinous thin tendons that upon breakup were converted to very small droplets. Similar small droplets are evident on the platelets in Fig. 15.

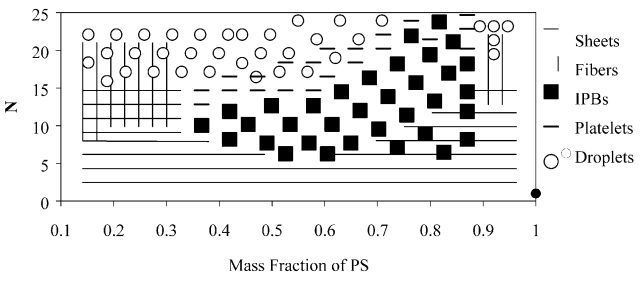

Fig. 16. Diagram indicating relation among predominant morphologies.

3.5. Morphology diagram

In order to summarize conditions and show associations for the wide variety of morphologies obtained in 31 samples, the morphology diagram in Fig. 16 was constructed in terms of N and composition. The presence of multiple morphologies for some conditions reflected somewhat differing rates for morphology development and also partial morphology transitions. Sheets formed initially at all compositions. In the range 35–90% PS, hole formation in sheets led to IPBs. In some cases, regions of sheets and IPBs were both present in the chaotic mixing cavity with the relative abundance of sheets smaller at larger N. Dual phase continuity was lost as holes enlarged to give platelets. Outside the range for IPB formation, layer breakup was qualitatively different. Circular hole formation was suppressed. Instead, numerous long and parallel undulations developed in layers that broke to give fibers. Capillary instabilities and platelet breakup ultimately led to the formation of droplets, where the smallest droplets had diameters related to the thicknesses of platelet fragments or fibers. Fig. 16 suggests that a variety of blend morphologies can be produced controllably at specific compositions. For example, at 60% PS, blends were obtained for different N with a predominant sheet, interpenetrating, platelet, or droplet morphology. This ability to produce blends with distinctly different morphologies at the same composition can be useful in studies of structure–property relationships.

4. Conclusions

In this study, the ability to gradually and deliberately evolve shapes among immiscible polymer components by chaotic mixing was investigated at various compositions. At all compositions, components were initially stretched and folded about one another due to kinematical effects associated with chaotic advection to give multiple layers. After additional processing time at intermediate compositions,

layer interactions and local differences in stretching and folding rates yielded localized thickness variations. Various types of hole formation and growth were found to play a central role in morphology development. Holes formed at locations in layers where thickness was smallest and enlarged preferentially in the direction of least thickness. Hole formation occurred interactively in the multilayer blends such that phase continuity occurred among previously separated layers. Layered morphologies yielded interpenetrating blends over a broad compositional range. Hole enlargement subsequently caused layers to fragment into abundant platelets to give blends with single phase continuity. Outside the range for interpenetrating blend formation, thickness variations in layers were less localized. Line ruptures or very highly elongated holes in the layers arose to give fiber shapes. In some cases, novel encapsulated structures were formed. With additional chaotic mixing, droplets were obtained with diameters similar to the parent layer thicknesses. It is noteworthy that the number and thickness of layers as well as the extent of hole growth were controllable by specification of chaotic mixing parameters. This ability to mix, control the extent of breakup, and select morphology with chaotic mixing devices provides special opportunities for investigating relationships among processing conditions, structure, and properties. Chaotic mixing when implemented in continuous flow modes may also be a basis for new automated blending devices where processing conditions can be adjusted on-line to obtain target morphologies.

Acknowledgements

Financial support was provided by the Engineering Research Center Program of the National Science Foundation under Award No. EEC-9731680. The authors express their appreciation to O. Kwon for assisting with the initial experiments. Concept illustrations were prepared by Nicholas A. Lamb.

References

[1] Aref H. J Fluid Mech 1984;143:1.
[2] Ottino JM. Kinematics of mixing: stretching, chaos and transport. Cambridge: Cambridge University Press, 1989.
[3] Zhang DF, Zumbrunnen DA. J Fluid Engng 1996;118:40.
[4] Leong CW, Ottino JM. J Fluid Mech 1989;209:463.
[5] Chien WL, Rising H, Ottino JM. J Fluid Mech 1986;170:355.
[6] Zumbrunnen DA, Miles KC, Liu YH. Composites, Part A 1996;27A:37.
[7] Danescu RI, Zumbrunnen DA. J Thermoplast Compos Mater 1998;11:299.
[8] Zumbrunnen DA, Inamdar S. Chem Engng Sci 2001;56:3893.
[9] Jones SW, Thomas OM, Aref H. J Fluid Mech 1989;209:335.
[10] Bigio DI, Young D. Polym Engng Sci 1993;33:1271.
[11] Zumbrunnen DA. J Textile Inst, Part 3 2000:92.
[12] Liu YH, Zumbrunnen DA. Polym Compos 1996;17:187.
[13] Liu YH, Zumbrunnen DA. J Mater Sci 1999;34:1701.
[14] Teh JW, Rudin A. Polym Engng Sci 1991;31:1033.
[15] Sundararaj U, Dori Y, Macosko CW. Polymer 1995;36:1957.
[16] Scott CE, Macosko CW. Polymer 1995;36:461.
[17] Schreiber HP, Olguin A. Polym Engng Sci 1983;23:129.
[18] Karger-Kocsis J, Kallo A, Kuleznev VN. Polymer 1984;25:279.
[19] Favis BD, Therrien D. Polymer 1991;32:1474.
[20] Miles KC, Nagarajan B, Zumbrunnen DA. J Fluid Engng 1995;117:582.
[21] Stokes JR, Boger DV. Phys Fl 2000;12:1411.
[22] Stone HA. Annu Rev Fluid Mech 1994;26:65.
[23] Zhang DF, Zumbrunnen DA, Liu YH. AIChE J 1998;44:442.
[24] Sanchez IC. Polym Engng Sci 1984;24:79.
[25] Willemse RC, Boer AP, Van Dam J, Gotsis AD. Polymer 1998;39:5879.
[26] Ma M, Vijayan K, Hiltner A, Baer E. J Mater Sci 1990;25:2039.
[27] Kwon O, Zumbrunnen DA. J Appl Polym Sci 2001;82:1569.
[28] Reiter G. Langmuir 1993;9:1344.
[29] Miles IS, Zurek A. Polym Engng Sci 1988;28:796.
[30] Benderly D, Siegmann A, Narkis M. Polym Compos 1996;17:86.
[31] Wiggins S. Chaotic transport in dynamical systems. New York: Springer, 1992. p. 17–73.
[32] Taylor GI, Michael DH. J Fluid Mech 1973;58:625.
[33] Sferrazza M, Heppenstall-Butler M, Cubitt R, Bucknall D, Webster J, Jones RAL. Phys Rev Lett 1998;81:5173.
[34] Kheshgi HS, Scriven LE. Chem Engng Sci 1991;46:519.
[35] Vaynblat D, Lister JR, Witelski TP. Phys Fluids 2001;13:1130.
[36] Inamdar S. MS Thesis. Clemson University; 2001.
[37] Taylor GI. Proc Res Soc Lond 1934;A146:501.